

Nonlinear Atom-Photon Interaction Induced Population Inversion and Inverted Quantum Phase Transition of Bose-Einstein Condensate in an Optical Cavity

Xiuqin Zhao,^{1,2} Ni Liu,³ and J-Q, Liang^{1,*}

¹*Institute of Theoretical Physics, Shanxi University, Taiyuan, Shanxi 030006, China*

²*Department of Physics, Taiyuan Normal University, Taiyuan, Shanxi 030001, China*

³*School of Physics and Electronic Engineering, Shanxi University, Taiyuan, Shanxi 030006, China*

In this paper we explore the rich structure of macroscopic many-particle quantum states for Bose-Einstein condensate in an optical cavity with the tunable nonlinear atom-photon interaction [Nature (London) 464, 1301 (2010)]. Population inversion, bistable normal phases and the coexistence of normal-superradiant phases are revealed by adjusting of the experimentally realizable interaction strength and pump-laser frequency. For the negative (effective) cavity-frequency we observe remarkably an inverted quantum phase transition (QPT) from the superradiant to normal phases with the increase of atom-field coupling, which is just opposite to the QPT in the normal Dicke model. The bistable macroscopic states are derived analytically in terms of the spin-coherent-state variational method by taking into account of both normal and inverted pseudospin states.

PACS numbers: 03.75.Mn, 71.15.Mb, 67.85.Pq

I. INTRODUCTION

Quantum phase transition (QPT), which exhibits the properties of quantum correlations, has become an exciting research field in many-body physics and also has important applications in quantum information processing. The Dicke model (DM) [1], which shows collective phenomena in a light-matter system [2, 3], is of particular interest for the study of the fascinating QPT, since it exhibits a second-order phase transition from a normal phase (NP) with zero average photon-number to the superradiant phase (SP) with non-zero photons predicted long ago [4, 5] and has broad application range [6]. The collective effects give rise to intriguing many-body phenomena such as the existence of a coherent SP at zero temperature [7]. Although the model itself is quite simple, it displays a rich variety of the unique aspects of quantum theory and has become a paradigmatic example of collective quantum behaviors. The DM Hamiltonian for the interaction of an ensemble of N identical two-level atoms with single mode of the electromagnetic field is written by [7, 8]

$$H_D = \omega_f a^\dagger a + \omega_a J_z + \frac{g}{2\sqrt{N}} (a^\dagger + a) (J_+ + J_-), \quad (1)$$

with $\hbar = 1$, where ω_a is the frequency difference between the two atomic levels, ω_f is the frequency of the cavity-field mode, and g is the atom-field dipole coupling strength. The boson operators a , a^\dagger are the annihilation and creation operators for the field, and the pseudospin J_i ($i = z, \pm$) is the collective atomic operator satisfying the angular momentum commutation relation: $[J_\pm, J_z] = \mp J_\pm$, $[J_+, J_-] = 2J_z$ with the spin length $j = N/2$. The model, being a classic problem

in quantum optics, continually provides a fascinating avenue of research in a variety of contexts. This is because the DM is a striking example for the macroscopic many-particle quantum state (MMQS), which can be solved rigorously. The QPT occurs at the critical coupling strength $g_c = \sqrt{\omega_f \omega_a}$ and the system enters a SP [7] when $g > g_c$. A significant achievement is the experimental study of the quantum behaviors of Bose-Einstein condensates (BECs) in ultrahigh-finesse optical cavities [2, 9]. More recently the time-dependent nonequilibrium experiments were performed in an open cavity [10, 11], which lead to the theoretical interpretations of nonequilibrium QPT [12–16].

It is believed that the QPT can take place only if the collective atom-photon coupling strength is the same order of the energy separation between the two atomic levels, which was considered as a challenging transition-condition. In the strongly coupled regime of cavity quantum electrodynamics (QED) this condition is shown to be accessible with the pump laser [8]. For a BEC in a high-finesse optical cavity, the energy space of two levels can be adjusted to be small enough and the QPT, namely the superradiance transition, has been observed experimentally [9]. This is achieved by introducing two optical Raman transitions in a four-level atomic ensemble along with the controlling of the pump laser power [13]. It is shown that the theoretical model Hamiltonian in relation with this experiment possesses a nonlinear atom-photon interaction resulted from the dispersive shift of cavity frequency [11]. For a weak nonlinear interaction, the onset of self-organization for the ultracold atoms can be used to detect the normal-superradiant QPT in the blue detuning of cavity frequency [11, 17]. This system of BEC in a high-finesse optical cavity has been regarded as a promising platform to explore the exotic many-body phenomena from atomic physics to quantum optics in a well-controlled way [2, 9, 18–28]. Since the magnitude of this nonlinear interaction can arrive at the same order as those of the detuning of cavity frequency and the col-

*Electronic address: jqliang@sxu.edu.cn

lective coupling strength, the QPT from NP to SP has been observed successfully [11]. Besides its applications in practical experiments the model of nonlinear atom-photon interaction itself is of theoretical interest. A natural question is whether or not the nonlinear interaction can lead to new MMQSs compared with the standard DM of Eq. (1). It has been shown that the nonlinear interaction, indeed, results in dynamically unstable phase [16]. Most recently the coexistence of NP and SP was found in the nonequilibrium QPT with time-dependent atom-field coupling [12, 16] based on the numerical simulation of zero-points of the energy functional. In order to understand the mechanism of multiphase coexistence we revisit the generalized Dicke model of BEC-cavity experiment [14, 17] with nonlinear interaction $J_z a^\dagger a$ in the whole region of experimental parameters to reveal the bistable NPs as well as the coexistence of NP and SP.

The Holstein-Primakoff (HP) transformation, which converts the pseudospin J_i (i.e. the collective atomic operators) into a one-mode bosonic operator, is the starting point for the most theoretical analysis of the QPT in relation with the DM. In the thermodynamic limit ($N \rightarrow \infty$) the DM reduces to two-mode boson Hamiltonian, the ground state of which can be obtained in terms of variational method with the help of bosonic coherent states [7, 17, 29–32]. We in this paper adopt the direct product of optical and spin coherent states (SCS) [33–35] as a trial wave function firstly proposed in Ref. [36] to achieve the energy functional. Based on the SCS variational method we are able to obtain the analytical expressions of MMQSs, energy spectra, atomic population and the photon number distribution as well. A full phase diagram with the multistable MMQSs are presented in the whole region of experimental parameters.

II. HAMILTONIAN FOR BEC IN A OPTICAL CAVITY WITH NONLINEAR INTERACTION AND ANALYTIC SOLUTIONS

Following the Refs. [12, 28, 37], we consider the system of four-level atomic ensemble in a high-finesse optical cavity with transverse pumping depicted in Fig. 1, where the transverse pumping laser of frequency ω_p creates a standing-wave potential and the ultracold atoms coherently scatter pump light into the cavity mode with a position-dependent phase.

Two excited states can be eliminated adiabatically and thus we have the effective two-level system. In an optical cavity all ultracold atoms are assumed to couple identically with the single-mode field and the system reduces to an extended DM given by [12, 17].

$$H = \omega a^\dagger a + \omega_a J_z + \frac{g}{2\sqrt{N}} (a^\dagger + a) (J_+ + J_-) + \frac{U}{N} J_z a^\dagger a, \quad (2)$$

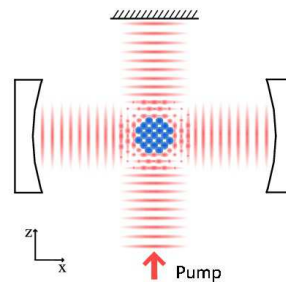


FIG. 1: (Color online) The experimental setup for a trapped BEC in an optical cavity with a transverse pumping laser to control the cavity frequency.

where

$$\omega = \Delta + \beta U, \quad (3)$$

is the effective cavity frequency with

$$\Delta = \omega_f - \omega_p,$$

being the pump-cavity field detuning and β is an experimental constant [12, 37]. The nonlinear atom-photon interaction U arising from the dispersive shift of cavity frequency [11, 14], can be both positive and negative values. The collective coupling strength g is tunable in experiment by varying the pump laser power [12]. The Hamiltonian Eq. (2) reduces to the standard DM Eq. (1) when the nonlinear interaction is absent. Since the effective frequency ω can be turned from positive to negative regions by the pump-cavity field detuning Δ and the atom-photon interaction constant U , much more rich phases arise compared with the ordinary DM.

We reinvestigate the MMQSs and related QPT based on the SCS variational method with advantage that both the normal (\Downarrow) and inverted (\Uparrow) pseudospin states revealed in the dynamic study [13] can be taken into account in order to see the multiple steady states observed in the nonequilibrium QPT [13, 14, 16]. Moreover, an energy functional with one-parameter only can be obtained and thus the stability of MMQSs is justified rigorously.

A. Spin coherent-state variational method

We begin with the average of Hamiltonian Eq. (2) in the optical coherent state $|\alpha\rangle$

$$H_{sp}(\alpha) = \langle \alpha | H | \alpha \rangle = \omega \gamma^2 + \omega_a J_z + \frac{U}{N} J_z \gamma^2 + \frac{g\gamma \cos \eta}{\sqrt{N}} (J_+ + J_-), \quad (4)$$

where α is the complex eigenvalue of photon annihilation operator a such that $a|\alpha\rangle = \alpha|\alpha\rangle$ and can be generally expressed as

$$\alpha = \gamma e^{i\eta}.$$

The effective spin Hamiltonian $H_{sp}(\alpha)$ possesses two macroscopic eigenstates namely the SCSs $|\mathbf{n}_{\mp}\rangle$ of south and north pole gauges respectively, which correspond to the normal (\Downarrow) and inverted (\Uparrow) pseudospin states in the dynamics of nonequilibrium DM [13]. The SCSs can be generated from the maximum Dicke states $|j, \pm j\rangle$ ($J_z|j, \pm j\rangle = \pm j|j, \pm j\rangle$) with the SCS transformation [15, 38], such that

$$|\mathbf{n}_{\pm}\rangle = R(\mathbf{n})|j, \pm j\rangle,$$

where the unitary operator is explicitly given by

$$R(\mathbf{n}) = e^{\frac{\theta}{2}(J_+e^{i\phi} - J_-e^{-i\phi})}. \quad (5)$$

As a matter of fact the SCSs of north and south pole gauges are actually the eigenstates of the spin projection operator $\mathbf{J} \cdot \mathbf{n}|\mathbf{n}_{\pm}\rangle = \pm j|\mathbf{n}_{\pm}\rangle$, where $\mathbf{n} = (\sin\theta\cos\phi, \sin\theta\sin\phi, \cos\theta)$ is the unit vector with the directional angles θ and ϕ . In the SCS the spin operators satisfy the minimum uncertainty relation, for example, $\Delta J_+ \Delta J_- = \langle J_z \rangle / 2$ and therefore the SCSs $|\mathbf{n}_{\pm}\rangle$ are called the macroscopic quantum states. The two macroscopic eigenstates of north and the south pole gauges are orthogonal i.e. $\langle \mathbf{n}_+ | \mathbf{n}_- \rangle = 0$. It is the key point to take into account of the both macroscopic eigenstates $|\mathbf{n}_{\pm}\rangle$ for revealing the multistable phases. Using the unitary transformations $R(\mathbf{n})$ for the spin operators J_z, J_+, J_-

$$\begin{aligned} \widetilde{J}_z &= J_z \cos\theta + \frac{1}{2} \sin\theta (J_+e^{-i\phi} + J_-e^{i\phi}), \\ \widetilde{J}_+ &= J_+ \cos^2\frac{\theta}{2} - J_-e^{2i\phi} \sin^2\frac{\theta}{2} - J_z e^{i\phi} \sin\theta, \\ \widetilde{J}_- &= J_- \cos^2\frac{\theta}{2} - J_+e^{-2i\phi} \sin^2\frac{\theta}{2} - J_z e^{-i\phi} \sin\theta, \end{aligned}$$

where $\widetilde{J}_z = R^\dagger(\mathbf{n})J_zR(\mathbf{n})$ etc., the effective spin Hamiltonian $H_{sp}(\alpha)$ is diagonalized under the conditions:

$$\begin{aligned} \Phi \sin\theta e^{i\phi} + \frac{g\gamma}{\sqrt{N}}(\cos^2\frac{\theta}{2} - e^{2i\phi} \sin^2\frac{\theta}{2}) \cos\eta &= 0, \\ \Phi \sin\theta e^{-i\phi} + \frac{g\gamma}{\sqrt{N}}(\cos^2\frac{\theta}{2} - e^{-2i\phi} \sin^2\frac{\theta}{2}) \cos\eta &= 0, \end{aligned} \quad (6)$$

with $\Phi = \frac{\omega_a}{2} + \frac{U}{2N}\gamma^2$. From the above conditions Eq. (6) the angle parameters θ, ϕ can be determined in principle. Thus we obtain the energy functional for the normal (\Downarrow) and inverted (\Uparrow) states respectively

$$E_{\mp}(\alpha) = \langle \mathbf{n}_{\mp} | H_{sp} | \mathbf{n}_{\mp} \rangle = \omega\gamma^2 \mp \frac{N}{2}A(\alpha, \theta, \phi), \quad (7)$$

where

$$A(\alpha, \theta, \phi) = \left(\omega_a + \frac{U}{2N}\gamma^2 \right) \cos\theta - \frac{2g}{\sqrt{N}} \sin\theta \cos\eta \cos\phi.$$

The desired MMQSs

$$|\psi_{\mp}\rangle = |\alpha\rangle |\mathbf{n}_{\mp}\rangle$$

and corresponding energies are found as local minima of the energy functional $E_{\mp}(\alpha)$.

B. Energy functions, atomic population and mean photon numbers

Using the diagonalization conditions Eq. (6) to eliminate the parameters $\cos\eta$ and $\cos\phi$, we obtain

$$\cos\theta = \frac{(\omega_a + \frac{U}{N}\gamma^2)}{A(\gamma)},$$

where the function $A(\alpha, \theta, \phi)$ in the energy functional Eq. (7) becomes a one-parameter function only

$$A(\gamma) = \sqrt{\omega_a^2 + \frac{2}{N}(\omega_a U + 2g^2)\gamma^2 + \frac{U^2}{N^2}\gamma^4}.$$

The energy functional Eq. (7) reduces after a tedious algebra to that of one variable i.e. $\gamma = |\alpha|$

$$E_{\mp}(\gamma) = \omega\gamma^2 \mp \frac{N}{2}A(\gamma), \quad (8)$$

which is a key point of our approach. The MMQS solutions are found from the usual extremum condition of the energy function

$$\frac{\partial E_{\mp}}{\partial \gamma} = \gamma \left[2\omega \mp \frac{(\omega_a + \frac{U}{N}\gamma^2)U + 2g^2}{A(\gamma)} \right] = 0. \quad (9)$$

The extremum condition Eq. (9) possesses always a zero photon-number solution $\gamma = 0$, which gives rise to the NP ($\gamma_{n_{\mp}} = 0$) only if it is stable with the positive second-order derivative, namely

$$\frac{\partial^2 E_{\mp}(\gamma_{n_{\mp}} = 0)}{\partial \gamma^2} = 2\omega \mp \left(U + \frac{2g^2}{\omega_a} \right) > 0. \quad (10)$$

We denote the NP states $\gamma_{n_{\mp}} = 0$ by N_{\mp} respectively. The non-zero photon-number solutions are found as

$$\gamma_{s_{\mp}}^2 = \frac{N}{U^2} \left[-(2g^2 + U\omega_a) \pm \frac{4g|\omega|}{\varsigma} \sqrt{\xi\varsigma} \right], \quad (11)$$

where

$$\xi = g^2 + U\omega_a, \quad \varsigma = 4\omega^2 - U^2.$$

The second-order derivative in the solutions $\gamma_{s_{\mp}}^2$ is also derived analytically

$$\frac{\partial^2 E_{\mp}(\gamma_{s_{\mp}}^2)}{N\partial \gamma^2} = \pm \varsigma \sqrt{\frac{\xi}{\xi}} \frac{\gamma_{s_{\mp}}^2}{g}. \quad (12)$$

The SPs denoted by S_{\mp} are realized from both positive photon-number Eq. (11) and the second-order derivative Eq. (12). Substituting the nonzero photon solutions Eq. (11) back to the extremum condition Eq. (9), it is easy to find the necessary conditions

$$\omega > 0, \quad \varsigma > 0, \quad (13)$$

and

$$\omega < 0, \quad \varsigma < 0, \quad (14)$$

to be fulfilled respectively for the normal state (\Downarrow) solution γ_{s-}^2 , and the inverted state (\Uparrow) γ_{s+}^2 . The normal state solution γ_{s-}^2 reduces exactly to that of DM at the limit $U \rightarrow 0$. While the solution γ_{s+}^2 for the inverted state (\Uparrow) is only possible when $U \lesseqgtr 0$ and thus is induced by the nonlinear interaction only. The critical lines can be fixed from the equations

$$\frac{\partial E_{\mp}(\gamma = 0)}{\partial \gamma} = 0,$$

which lead to the phase boundaries

$$g_{c\mp} = \sqrt{\left(\pm\omega - \frac{U}{2}\right)\omega_a}. \quad (15)$$

When $U = 0$, the critical pint for the normal state (\Downarrow) approaches the typical value of DM that $g_{c-} = \sqrt{\omega\omega_a}$, which is valid only for the positive effective frequency $\omega > 0$. Substituting the photon number obtained in Eq. (11) into the energy function Eq. (8) we achieve the mean energies of per atom for the SP

$$\begin{aligned} \varepsilon_{s\mp} &= \frac{E_{s\mp}}{N} = \frac{1}{U^2} \left[-(2g^2 + U\omega_a) \pm 4g\omega\sqrt{\frac{\xi}{\varsigma}} \right] \omega \\ &\mp g\sqrt{\frac{\xi}{\varsigma}}, \end{aligned} \quad (16)$$

which become at the critical lines $g_{c\mp}$

$$\varepsilon_{s\mp}(\gamma_{s\mp}^2 = 0) = \mp \frac{\omega_a}{2},$$

for the normal (\Downarrow) and inverted (\Uparrow) states respectively. The mean photon number of SP in the wave functions $|\psi_{\mp}\rangle$ is obviously

$$n_{p\mp} = \frac{\langle \psi_{\mp} | a^\dagger a | \psi_{\mp} \rangle}{N} = \gamma_{s\mp}^2, \quad (17)$$

while the atomic population imbalance becomes

$$\Delta n_{a\mp} = \frac{\langle \psi_{\mp} | J_z | \psi_{\mp} \rangle}{N} = \frac{1}{U} \left[-|\omega| \pm \frac{g}{2} \sqrt{\frac{\varsigma}{\xi}} \right], \quad (18)$$

which reduces to the well known values

$$\Delta n_{a\mp}(\gamma_{s\mp}^2 = 0) = \mp \frac{1}{2},$$

at the critical lines $g_{c\mp}$. A full atomic population inversion i.e. $\Delta n_a = 1/2$ is found in the inverted state (\Uparrow). It may be worth while to remark that all these formula for the normal state (\Downarrow) reduce to those in the standard DM when $U \rightarrow 0$ and $\omega = \omega_f$ in Hamiltonian (2), where the critical point of QPT is the well known form $g_c = \sqrt{\omega_f\omega_a}$.

III. BISTABILITY AND ATOMIC POPULATION INVERSION

We have presented in the previous section the general formula and now show the particular MMQs in the experimental parameter-values. Following the experiment [11] the nonlinear interaction value spreads in a wide region $U \in (-80 \sim 80) MHz$ (the unit of energy and frequency is MHz throughout the paper) with the atomic frequency $\omega_a = 1$ and the collective atom-field coupling strength $g \in (0 \sim 10)$. We first consider the blue detuning of the pump-cavity field $\Delta = -20$. With the experimental constant [37] $\beta = 7/6$, the effective frequency becomes

$$\omega = (-20 + \frac{7U}{6}). \quad (19)$$

The phase boundary for the normal state (\Downarrow) is found from Eq. (15)

$$g_{c-} = \sqrt{2(-10 + \frac{U}{3})}, \quad (20)$$

which increases with the nonlinear interaction U in exact agreement with the previous observation [37]. Below g_{c-} we have only the phase N_- shown in Fig. 2. The SP of S_- exists in the region of $g > g_{c-}$ and $U > 30$ (the value can be also evaluated from the necessary condition Eq. (13) i.e. $\varsigma > 0$). The phase boundary for the inverted state (\Uparrow) obtained from Eq. (15) is

$$g_{c+} = \sqrt{5(4 - \frac{U}{3})}, \quad (21)$$

which increases with the decreasing U as shown in Fig. 2. The NP of N_+ for the inverted state (\Uparrow) always exists above the boundary curve g_{c+} , so that we have the bistable NPs denoted by $NP_{bi}(N_-, N_+)$ in Fig. 2, in which N_- with the lower energy is the ground state. Correspondingly the notation $SP_{co}(S_-, N_+)$ means the SP of S_- coexisting with N_+ since S_- is the lower energy state. The bistable MMQs observed in this paper agree with the dynamic study of nonequilibrium QPT [13, 16].

In the area (yellow) between the line of $U = 30$ and curve g_{c+} we have only the single NP of N_+ with full population inversion, which induced by the nonlinear interaction is a new observation. The SP of S_+ for the inverted state (\Uparrow) does not exist, since the necessary condition Eq. (14) can not be fulfilled in the blue detuning. Below the phase boundary g_{c+} the zero photon-number solution ($\gamma = 0$) is unstable with negative second-order derivative Eq. (10) and we call it the unstable macroscopic vacuum (UMV). The QPT in DM is characterized by the average photon number n_p (or γ), which serves as an order-parameter, with $n_p > 0$ for the SP and $n_p = 0$ in the NP. In Fig. 3 we present the average photon number n_p (a), atomic population imbalance Δn_a (b) between the two atom-levels, and the average energy ε (c) as a function of the atom-field coupling strength g , where (black) solid

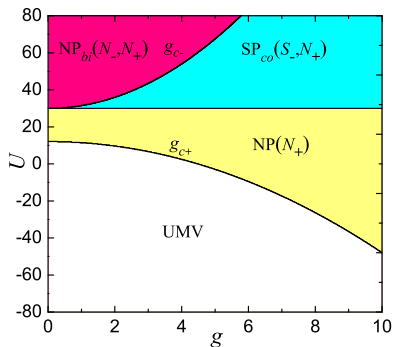


FIG. 2: (Color online) Phase diagram in blue detuning with $\Delta = -20$. $\text{NP}_{bi}(N_-, N_+)$ indicates the bistable NPs and $\text{SP}_{co}(S_-, N_+)$ means the SP of S_- coexisting with N_+ . The single NP of N_+ with full population inversion is located between the line of $U = 30$ and phase boundary g_{c+} . The unstable macroscopic vacuum (UMV) is found under the curve g_{c+} .

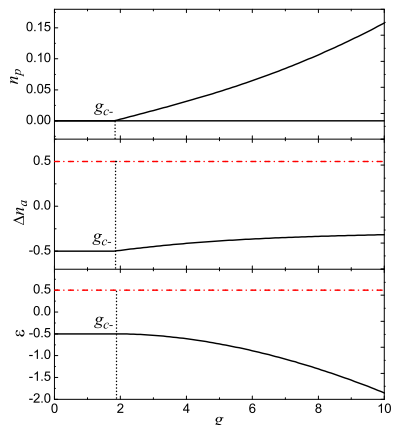


FIG. 3: (Color online) The variations of average photon number n_p (a), population imbalance Δn_a (b) and average energy ε (c) with respect to the coupling constant g for $U = 35$ in the blue detuning of $\Delta = -20$, with (black) solid lines for the normal state (\Downarrow), (red) dot and dash lines for the inverted state (\Uparrow). The critical point of QPT from NP of N_- to the SP of S_- is $g_{c-} = \sqrt{10/3}$ in the given U value.

lines are for the normal state (\Downarrow) and (red) dot and dash lines for the inverted state (\Uparrow) throughout the paper.

The QPT from NP of N_- to SP of S_- is the standard DM type, while the nonlinear interaction U only shifts the critical point g_{c-} toward the higher value direction of the atom-field coupling g [37]. For the given value of $U = 35$ in Fig. 3 the critical point of QPT can be evaluated precisely for the Eq. (20) that $g_{c-} = \sqrt{10/3}$. The NP of N_+ remains not changed through the critical point g_{c-} , so that it is the bistable $\text{NP}_{bi}(N_-, N_+)$ below g_{c-} while the coexistence phase of $\text{SP}_{co}(S_-, N_+)$.

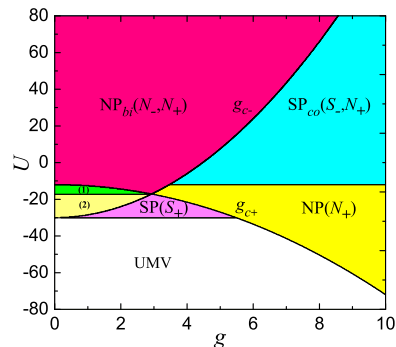


FIG. 4: (Color online) Phase diagram in red detuning with $\Delta = 20$. The SP of S_+ for the inverted state (\Uparrow) appears when the effective frequency becomes negative $\omega < 0$. (1) indicates the single NP of N_- , (2) is for $\text{NP}_{co}(N_-, S_+)$.

IV. INVERTED QUANTUM PHASE TRANSITION

It is an interesting aspect of the nonlinear interaction to see whether or not the SP of S_+ for the inverted state can be realized in the practical experiment. To this end we now turn to the red detuning ($\omega_p < \omega_f$) with, for example, $\Delta = 20$. The phase boundary lines are respectively found from Eq. (15) as

$$g_{c-} = \sqrt{2\left(10 + \frac{U}{3}\right)}, \quad (22)$$

and

$$g_{c+} = \sqrt{-5\left(4 + \frac{U}{3}\right)}, \quad (23)$$

showing in Fig. 4. Two lines cross at the point $g_{c-} = g_{c+}$ ($U = -120/7$), which appears as a critical point of multiple phases. The SP of S_- with $\gamma_{s-}^2 > 0$ coexists with the NP of N_+ in the region of $g > g_{c-}$ and $U > -12$ determined from the necessary condition Eq. (13) (cyan area in Fig. 4). The the bistable $\text{NP}_{bi}(N_-, N_+)$ is located in the area for $g \leq g_{c-}$ (pink area in Fig. 4). The single NP of N_+ with full atomic population inversion is bounded by the line of $U = -12$ and the critical curves g_{c-} , g_{c+} (the yellow area in Fig. 4). The label (1) indicates a small region of the single NP of N_- . The SP of S_+ with the stable solution of $\gamma_{s+}^2 > 0$ is found in the region of $U > -30$ and $U < -17$ when $g < g_{c+}$, which is below the critical boundary line g_{c+} just opposite to the normal state (\Downarrow) case. The notation $\text{NP}_{co}(N_-, S_+)$ marked by label (2) in Fig. (4) means the NP of N_- coexisting with S_+ since N_- is the lower energy state.

The QPT from NP to SP for the standard DM is along the increasing direction of coupling constant g , while the QPT in the inverted state (\Uparrow) would be in the opposite direction seen from the phase diagram in Fig. 4, where the SP of S_+ is located on the left-hand side of

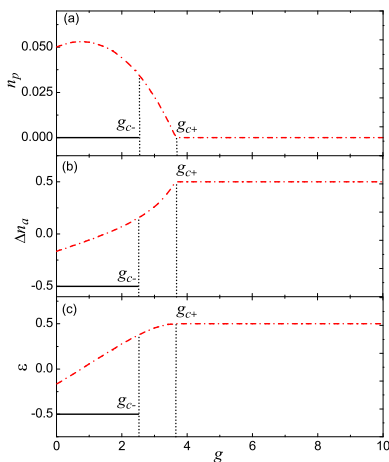


FIG. 5: (Color online) n_p (a), Δn_a (b), and ε (c) curves in red detuning for $U = -20$. The QPT from NP of N_+ to the SP of S_+ is in the inverted direction.

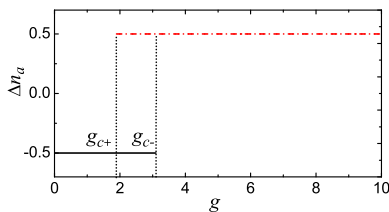


FIG. 6: (Color online) The QPT among NPs of different types showing by the variation of atomic population imbalance Δn_a for $U = -14$.

the critical line g_{c+} . Fig. 5 displays the curves of average photon number n_p (a), atomic population imbalance Δn_a (b), and the energy ε (c) for $U = -20$. The critical point $g_{c-} = 2\sqrt{5/3}$ separates the coexistence phase of NP $_{co}(N_-, S_+)$ and the single SP of S_+ . Then with the increase of g the SP of S_+ transits to NP of N_+ at the critical point $g_{c+} = 2\sqrt{10/3}$. The QPT from the SP of S_+ to the NP of N_+ is just in the inverted direction compared with standard DM. One should not be so surprised by this inverted QPT, since the effective frequency is negative $\omega < 0$ in the region, where the the SP of S_+ exists. By adjusting the nonlinear constant, for example $U = -14$, the QPT among NPs of different types can be also realized, which is displayed in Fig. 6. The transition from NP of N_- to bistable NP $_{bi}(N_-, N_+)$ takes place at the critical point $g_{c+} = \sqrt{10/3}$ [de-

termined from Eq. (23)] and then the transition from bistable NP $_{bi}(N_-, N_+)$ to the NP of N_+ follows at the critical point $g_{c-} = 4\sqrt{2/3}$ [obtained from Eq. (22)]. Even though the order-parameter is zero $n_{p\mp} = 0$ in both sides of critical point, while ground state structure changes.

V. CONCLUSION AND DISCUSSION

The system of BEC in an optical cavity provides a marvelous model for reveal of QED theory. Although having investigated extensively the new phenomena emerge surprisingly, among which the population inversion with full occupation of excited state and inverted QPT are most exciting. The bistable MMQSs can be observed experimentally by tuning the frequency of pump laser and the atom-photon interaction strength, which play central roles in the observations. The SP of S_+ for the inverted pseudospin state (\uparrow) exists only when the effective frequency becomes negative $\omega < 0$ along with the nonzero atom-photon interaction. It should be noticed that when the interaction tends to zero $U \rightarrow 0$ the solutions for normal state (\downarrow) reduce exactly to those of the standard DM. We also remark that the SCS variational method has advantage in the theoretical investigation of macroscopic quantum properties of the atom-ensemble and cavity-field system, since it results in a one-parameter variational energy-function to achieve rigorously the analytic solutions of the MMQS. More importantly the inverted pseudospin state (\uparrow) comes into the formulation in a natural way giving rise to the bistable phases, which predicted in the present paper are in agreement with the semiclassical dynamics of nonequilibrium DM [13]. They were also realized recently by two of us (N.L and J.Q.L) in a time-driving nonequilibrium model, where multiple local minima of energy functional are found by the numerical simulation [16].

ACKNOWLEDGEMENTS

This work is supported by the National Natural Science Foundation of China, under Grant No. 11275118 and the Research Training Program for Undergraduates of Shanxi University (Grant No 2014012174).

[1] R. H. Dicke, Phys. Rev. **93**, 99 (1954).
 [2] Y. Colombe, T. Steinmetz, G. Dubois, F. Linke, D. Hunger, and J. Reichel, Nature (London) **450**, 272 (2007).
 [3] O. Castaños, E. Nahmad-Achar, R. López-Peña, and J. G. Hirsch, Phys. Rev. A **86**, 023814 (2012).

[4] Y. K. Wang, and F. T. Hioe, Phys. Rev. A **7**, 831 (1973).
 [5] K. Hepp, and E. H. Lieb, Ann. Phys. (N. Y.) **76**, 360 (1973).
 [6] P. Zanardi, M. G. A. Paris, and L. Campus Venuti, Phys. Rev. A **78**, 042105 (2008).
 [7] C. Emary, and T. Brandes, Phys. Rev. E **67**, 066203

- (2003).
- [8] F. Dimer, B. Estienne, A. S. Parkins, and H. J. Carmichael, *Phys. Rev. A* **75**, 013804 (2007).
 - [9] F. Brennecke, T. Donner, S. Ritter, T. Bourdel, M. Köhl, and T. Esslinger, *Nature (London)* **450**, 268 (2007).
 - [10] K. Baumann, R. Mottl, F. Brennecke, and T. Esslinger, *Phys. Rev. Lett.* **107**, 140402 (2011).
 - [11] K. Baumann, C. Guerlin, F. Brennecke, and T. Esslinger, *Nature (London)* **464**, 1301 (2010).
 - [12] J. Keeling, M. J. Bhaseen, and B. D. Simons, *Phys. Rev. Lett.* **105**, 043001 (2010).
 - [13] M. J. Bhaseen, J. Mayoh, B. D. Simons, and J. Keeling, *Phys. Rev. A* **85**, 013817 (2012).
 - [14] V. M. Bastidas, C. Emary, B. Regler, and T. Brandes, *Phys. Rev. Lett.* **108**, 043003 (2012).
 - [15] Z. -D. Chen, J. -Q. Liang, S. -Q. Shen, and W. -F. Xie, *Phys. Rev. A* **69**, 023611 (2004).
 - [16] N. Liu, J. D. Li, and J. -Q. Liang, *Phys. Rev. A* **87**, 053623 (2013).
 - [17] D. Nagy, G. Kónya, G. Szirmai, and P. Domokos, *Phys. Rev. Lett.* **104**, 130401 (2010).
 - [18] R. Puebla, A. Relaño, and J. Retamosa, *Phys. Rev. A* **87**, 023819 (2013).
 - [19] J. Larson, B. Damski, G. Morigi, and M. Lewenstein, *Phys. Rev. Lett.* **100**, 050401 (2008).
 - [20] S. Morrison, and A. S. Parkins, *Phys. Rev. Lett.* **100**, 040403 (2008).
 - [21] J. M. Zhang, W. M. Liu, and D. L. Zhou, *Phys. Rev. A* **78**, 043618 (2008).
 - [22] G. Chen, X. Wang, J. -Q. Liang, and Z. D. Wang, *Phys. Rev. A*, **78**, 023634 (2008).
 - [23] J. Larson, and J. -P. Martikainen, *Phys. Rev. A* **82**, 033606 (2010).
 - [24] L. Zhou, H. Pu, H. Y. Ling, K. Zhang, and W. Zhang, *Phys. Rev. A* **81**, 063641 (2010).
 - [25] M. J. Bhaseen, M. Hohenadler, A. O. Silver, and B. D. Simons, *Phys. Rev. Lett.* **102**, 135301 (2009).
 - [26] A. O. Silver, M. Hohenadler, M. J. Bhaseen, and B. D. Simons, *Phys. Rev. A* **81**, 023617 (2010).
 - [27] G. Szirmai, D. Nagy, and P. Domokos, *Phys. Rev. Lett.* **102**, 080401 (2009).
 - [28] G. Szirmai, D. Nagy, and P. Domokos, *Phys. Rev. A* **81**, 043639 (2010).
 - [29] F. Persico, and G. Vetri, *Phys. Rev. A* **12**, 2083 (1975).
 - [30] G. Chen, J. Q. Li, and J. -Q. Liang *Phys. Rev. A* **74**, 054101 (2006).
 - [31] B. M. Garraway, *Phil. Trans. R. Soc. A* **369**, 1137-1155 (2011).
 - [32] N. S. Tonchev, J. G. Brankov, and V. A. Zagrebnov, *J. Optoelectron. Adv. Mater.* **11**, 1142-1149 (2009).
 - [33] J. M. Radcliffe, *J. Phys. A: Gen. Phys.* **4** 313 (1971).
 - [34] D. Markham, and V. Vedral, *Phys. Rev. A* **67**, 042113 (2003).
 - [35] A. Altland, and F. Haake, *New J. Phys.* **14**, 073011 (2012).
 - [36] O. Castaños, E. Nahmad-Achar, R. López-Peña, and J. G. Hirsch, *Phys. Rev. A*, **83**, 051601(R) (2011).
 - [37] N. Liu, J. L. Lian, J. Ma, L. T. Xiao, G. Chen, J.-Q. Liang, and S. T. Jia, *Phys. Rev. A*, **83**, 033601 (2011).
 - [38] Y. -Z. Lai, J. -Q. Liang, H. J. W. Müller-Kirsten, and J. G. Zhou, *Phys. Rev. A* **53**, 3691 (1996).